Accepted Manuscript

Tracing of anthropogenic zinc sources in coastal environments using stable isotope composition

Daniel F. Araújo, Geraldo R. Boaventura, Wilson Machado, Jerome Viers, Dominik Weiss, Sambasiva R. Patchineelam, Izabel Ruiz, Ana Paula C. Rodrigues, Marly Babinski, Elton Dantas
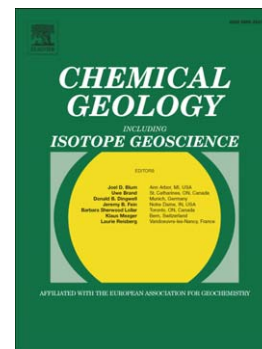
Please cite this article as: Araújo, Daniel F., Boaventura, Geraldo R., Machado, Wilson, Viers, Jerome, Weiss, Dominik, Patchineelam, Sambasiva R., Ruiz, Izabel, Rodrigues, Ana Paula C., Babinski, Marly, Dantas, Elton, Tracing of anthropogenic zinc sources in coastal environments using stable isotope composition, *Chemical Geology* (2016), doi: 10.1016/j.chemgeo.2016.12.004

Tracing of anthropogenic zinc sources in coastal environments using stable isotope composition

Daniel F. Araújo[a-b-1]; Geraldo R. Boaventura[a]; Wilson Machado[c]; Jerome Viers[b]; Dominik Weiss[d]; Sambasiva R. Patchineelam[c]; Izabel Ruiz[e]; Ana Paula C. Rodrigues[c]; Marly Babinski[e;] Elton Dantas[a;]

a. Universidade de Brasília, Instituto de Geociências, Campus Darcy Ribeiro, L2, Asa Norte, Brasília, Distrito Federal, Brazil.

b. Géosciences Environnement Toulouse (GET—UMR 5563 CNRS, Université Paul Sabatier, IRD), 14 Edouard Belin, 31400, Toulouse, France.

c. Universidade Federal Fluminense, Departamento de Geoquímica, Campus do Valonguinho, Niterói, Rio de Janeiro, Brazil.

d. Imperial College London, Earth Science and Engineering, London, United Kingdom

e. Universidade de São Paulo, Instituto de Geociências, Rua do Lago 562, Cidade Universitária, São Paulo, Brazil.

1-Corresponding author: Daniel F. Araújo: danielunb.ferreira@gmail.com, phone: +556135682760

Abstract

The use of zinc isotopes to trace anthropogenic sources in coastal areas has been tested in this study. We determined the stable isotopic composition of zinc in sediment cores, suspended particulate matter (SPM) and rocks collected at the Sepetiba Bay (southeastern Brazil), an estuarine lagoon heavily impacted by metallurgic activities. These isotopic signatures were compared with those from willemite ore, which represent the main mineral refined by the major industrial source of zinc. The aim was to test if this tracer system enables to identify sources and sinks of anthropogenic zinc and to reconstruct the temporal and spatial evolution of zinc contamination. The zinc isotopic compositions (expressed using the $\delta^{66}Zn$ notation relative to the JMC 3-0749-L solution) showed significant variations in the sediment cores, the SPM, and willemite ore minerals, ranging between -0.01 and +1.15‰. Spatial and temporal analysis of sediments samples fit well in a model of mixing involving three main end-members: i) Terrestrial background ($\delta^{66}Zn_{JMC} = +0.28 \pm 0.12$‰, 2σ); ii) marine detrital material ($\delta^{66}Zn_{JMC} = +0.45 \pm 0.03$‰, 2σ); and iii) a major anthropogenic source associated with electroplating wastes released into the bay ($\delta^{66}Zn_{JMC} = +0.86 \pm 0.15$‰, 2σ). Sediment cores collected in the mud flats showed high correlation between $\delta^{66}Zn$ and zinc enrichment factors, suggesting good preservation of the isotopic records of natural and anthropogenic sources. The sediment core sampled from a mangrove wetland located in a zone impacted by the metallurgy presented levels of zinc up to 4% (sediment dry weight) and preserved the isotopic signatures of electroplating wastes, despite evidences that post depositional processes slightly changed the isotopic signatures in some layers from this core toward heavier $\delta^{66}Zn_{JMC}$ values (above +1.0‰). A two component mixing model suggests contributions of this major anthropogenic Zn source up to nearly 80% during periods of electroplating activities. Our work suggests that Zn isotope compositions of sediments are reliable tracers of anthropogenic sources and, therefore, can be useful to improve environmental monitoring efforts in coastal systems.

Keywords: metal isotopes; stable isotopes; metal contamination; estuarine processes

1. Introduction

Coastal areas worldwide are under strong pressure from anthropogenic metal contamination as most of the global population and of economic activities are concentrated along the coasts and estuaries (Clark, 1996; Lewis et al., 2011). While numerous publications have associated the increase of metal fluxes in the coastal environments as evidences of human impacts, an accurate discrimination of natural and anthropogenic sources and identification of contaminant pathways remains a major concern (Abrahim and Parker, 2008; Bhardwaj et al., 2009; Lewis et al., 2011; Pan and Wang, 2012; Alves et al., 2014; Bastami et al., 2014; Kim et al., 2015; Marcovecchio et al., 2016), since the fate and mobility of metals is controlled by multiple factors, such as biologically-mediated changes in chemical speciation, sorption and desorption processes and hydrodynamic features (Langston, 1988; Turner; 1996; Bianchi, 2007; Du Laing et al., 2008; Mason, 2013).

In recent years, metal stable isotopes have been critically assessed as a tool to obtain qualitative and quantitative integrated information about sources, pathways and biogeochemical processes of these elements in the environment (Wiederhold, 2015). Of particular interest is the zinc isotope system, since zinc is a ubiquitous trace metal in the biosphere and geosphere, which is an essential micronutrient to organisms, but may be toxic in high concentrations (Adriano and Adriano, 2001). It is widely used in alloys, pesticides, electroplating and commonly associated to mining impacts due the economic importance of its ores (Hudson-Edwards et al., 2011, Gordon et al., 2013).

Previous work suggested that zinc isotopes fractionate during major anthropogenic process such as smelting (Shiel et al., 2010, Weiss et al., 2007), combustion (Matielli et al., 2007, Ochoa and Weiss, 2015) and electroplating (Kavner et al., 2008), generating anthropogenic fingerprints isotopically distinct from natural isotopic compositions (Guegien, 2008; Yin et al., 2016,). High-temperature processes involved during roasting and smelting of ores tend to fractionate zinc isotopes in the gas phase, with an enrichment of the lightest isotopes in air emissions and heavier isotopes in slags and effluents (Sonke et al., 2008; Borok et al., 2010; Ochoa Gonzalez and Weiss, 2015; Ocho Gonzalez et al., 2016; Yin et al., 2016). In contrast to these anthropogenic high temperature processes, geological high temperature processes including magmatic differentiation seems not produce significant isotopic fractionation resulting in a homogeneous zinc isotopic composition of the bulk Earth (Chen et al., 2013). The significant variation in the isotopic compositions derived of anthropogenic

sources compared to the natural background (soils and rocks, for example) suggest that zinc isotopes are a powerful tracer to discriminate and quantify several pollutant sources, such as vehicle emissions and tire wear (Gioia et al., 2008; Thapalia et al, 2010; Thapalia et al., 2015, Ochoa and Weiss, 2016), wastewaters and sewage (Chen et al., 2008; 2009), mining and metallurgy byproducts (Dolgopolova et al., 2006; Mattielli et al., 2006; Weiss et al., 2007; Sivry et al., 2008).

Critical appreciations of zinc isotopes as potential tracer of biogeochemical processes and sources in coastal environments remain scarce to date. In the Gironde fluvial-estuarine system (France), the isotopic composition of suspended particulate matter (SPM) did not distinguish anthropogenic and natural sources, possibly due to on-site remediation of the contamination source and the mixture with natural Zn in the fluvial-estuarine continuum (Petit et al., 2015). In the dissolved phase, the large isotopic variation observed was attributed to adsorption processes in the estuary gradient and maximum turbidity zone (MTZ) (Petit et al., 2015). Therefore, the applicability of Zn as tracer of metallurgical sources in coastal areas remains not conclusive, requiring additional investigations.

To this end, we conducted an in depth study of zinc isotopes in Sepetiba Bay, a lagoon-estuarine system located 60 km from Rio de Janeiro City, southeastern Brazil. This bay offers an ideal environment to apply zinc isotopes, since it presents well-known historical impacts of zinc contamination associated to old electroplating wastes. Moreover, its watershed hosts several potential zinc diffuse sources which include urban effluents, petrochemical, steelworks, plastic, rubber and food and beverage industries, and port activities that include sediment remobilization by dredging (Molisani et al., 2004). In this complex system, the stable isotopic composition of zinc was determined in five sediment cores, suspended particulate matter (SPM), rock and ore samples, with the aim of to develop new constraints on the use of a novel tracer for coastal areas to identify sources, pathways and sinks of anthropogenic zinc and hence to reconstruct the temporal and spatial evolution of zinc contamination.

2. Study area

Sepetiba Bay (Fig.1) is a 519-km^2, lagoon-estuary water body, with a wide intertidal area, including 40 km^2 of mangroves forests. At 60 km south of Rio de Janeiro City, this bay and its drainage basin host a large population, an expressive industrial park and

important harbor activity, implying significant economic importance (Leal Neto et al., 2006; Roncarati and Carelli, 2012).

The geology of the basin is composed of Quaternary sediments and granite-gneisses rocks (Roncarati and Carelli, 2012). In the northern and eastern parts of the bay, nine rivers drain an extensive watershed of approximately 2,654 km^2. The three main watercourses (Guandu, Guandu-Mirim and Guarda rivers) cross the industrial park by artificial channels and contribute more than >90% of watershed's total input of fresh water to the bay (Molisani et al., 2004; Roncarati and Carelli, 2012). The São Francisco channel, with an annual flow of 6.5 x 10^9 m^3, is responsible for over 86% of the total freshwater runoff input (Molisani et al., 2004). The extensive contribution of sediments to the bay coming from the rivers result in a wide range of sedimentation rates ranging between 0.12 to 1.3 cm per year (Smoak and Patchineelam, 1999; Molisani et al., 2004; Marques et al., 2006; Gomes et al., 2009). Water circulation in the bay is controlled by tides and the pattern of surface currents tends to clock direction (Leal Neto et al., 2006; Roncarati and Carelli, 2012). The lagoon hydrodynamics tend to deposit most part of sediments in the tidal flats and mangroves along the northeastern coastal area of the bay (Roncarati and Carelli, 2012; Montezuma, 2013).

The population of Sepetiba Bay drainage basin increased significantly from 600,000 to up 1.34 million in the last five decades, and in most part, under precarious conditions of basic sanitation (Leal Neto, 2006). Between the 1960s and 1990s, an electroplating plant operated close to the mangrove of Saco do Engenho (Fig.1), representing one of the main producers of zinc in Brazil, with a total capacity of 60.000 tons per year. The zinc purification process used silicate ores (calamine and willemite) acquired from Vazante deposit (Minas Gerais, Brazil), one of the most important deposits of zinc in Brazil. The ores were crushed and leached by sulfuric acid followed by filtration and purification of solution. The purified solution was then carried to electrolytic cells where the zinc plates were produced. After this, the plates underwent smelting and casting processes (Barone, 1973). The low production efficiency (75 to 90%) of this process contributed for the high production of wastes (Barcellos and Lacerda, 1994), that had inadequate contention.

The stack of wastes (estimated to about 600,000 tons, and containing about 200 tons of cadmium and 50,000 tons of zinc) were exposed to the open air and lixiviated by rainfall, reaching surrounding mangroves and the bay through a tidal creek located in the Saco do Engenho mangrove, which is the *hot spot* area (Fig.1) (Molisani et al.,

5

2004). The amount of pollutants remobilized from the wastes are estimated to about 24 t y^{-1} of cadmium and 3,660 t y^{-1} for Zn (Molisani et al., 2004). Zinc content in sediments of the bay (Pellegati et al., 2001; Wasserman et al., 2001), oysters (Rebelo et al., 2003; Larcerda and Molisani, 2006;) and brown algas (Amado Filho et al., 1999) often exceed 2,000, 80,000 and 800 µg g^{-1}, respectively. Cadmium reaches concentrations in sediments that are comparable to concentrations found in soils of sites with the historical Itai-itai disease outbreak (Kasuya et al., 1992). The stack of wastes was removed in 2012.

3. Materials and Methods

3.1 Sampling and sample preparation

Sediment cores were collected from five different locations within the Sepetiba Bay (Fig.1). Core T1 was sampled within a white mangrove (*Laguncularia racemosa*) stand, located into the Saco do Engenho tidal creek, representing the contamination hot spot due to the leaching process of the electroplating wastes and deposition in this area. The other cores were collected in subtidal or intertidal mud flats located along the inner bay areas. Core T2 was collected near the Saco do Engenho channel mouth, while core T3 was located near the mouth of the São Francisco channel. Core T4 was collected in Enseada das Garças, in a tidal flat located in the northeastern bay area, close to an ecological reserve with mangrove vegetation, but under the influence of anthropogenic activities, such as the discharge of untreated domestic sewage. In contrast to the cores collected close to the northeastern shore, the T5 core was collected near the Marambaia sandbank and the main communication of the bay with the open sea. All sediment cores were taken using 6 cm-diameter, 60 cm-length acrylic tubes, and sectioned in the field at 5 cm intervals. Each sub-sample was stored in polyethylene bags and kept frozen in thermal boxes with ice packs. The samples were dried at 40 ºC, crushed and sieved at 63 µm. This grain size fraction (< 63 µm) was used for elemental and isotopic analyses.

Sampling locations for suspended particulate matter (SPM) were chosen with the aim to characterize: 1) Fluvial material, which includes crustal materials and potential contaminants brought to the bay by the San Francisco and Guandu channels (R1 and R2 samples, Fig.1); 2) electroplating wastes transported by the creek that cross the Saco do Engenho's mangrove (SE samples, Fig.1); and 3) ocean detrital particulate matter that enters the bay to the west (B samples, Fig.1). The SPM samples from the rivers were

collected 6 km upstream during the low tide to represent best the fluvial inputs. Conductivity was controlled to guarantee the sampling in the fresh waters. Bottles for sampling were washed overnight in sub-boiling HCl and rinsed three times with pure water prior to using in the field. Following sample collection, between 150 and 500 ml of water was filtered using a through an acid cleaned 0.45 μm acetate cellulose membrane previously dried and weighted. Back in the laboratory, SPM samples were dried and weighed to calculate the mass of the suspended material.

Granite rock samples were collected around a quarry located at north of the Saco do Engenho mangrove. The rocks were split in two group and crushed. The two groups were pulverized separately, constituting two aliquots representative for the geology of the study area. Three willemite ores from the hypogene non-sulfide zinc deposit of Vazante Mine (Minas Gerais, Brazil) were used to represent the main mineral refined during the industrial electroplating process (Barone, 1973).

3.2. Sample treatment and elemental analysis

All reagents used for the samples digestion were prepared using > 18.2 MΩ H_2O (Nanop System®) and ultra-pure acids (Merck®) distillated by sub-boiling in Teflon stills. The chemical procedures for trace elements were performed under clean-air conditions and evaporations were conducted in clean boxes. The samples were weighed in Savillex® Teflon beakers with sample masses ranging from 20 to 100 mg (sediments, rocks and certified reference materials, i.e. BCR-2 and BHVO-2, USGS) and 5 to 10mg for willemite ores were digested on a hot plate using a multiple-step acid procedure with HF, HNO_3, HCl. Suprapur H_2O_2 30% (Merck®) was used to oxidize organic matter in some sediment samples. Subsequently, the samples were evaporated to dryness on a hot plate and 1 ml of concentrated HNO_3 was added to drive off the remaining HF. After, the samples were dissolved in 6 M HCl evaporated to dryness again and re-dissolved in 2 M HCl. This final solution was split in two aliquots for chemical separation of zinc and trace elements analysis, respectively. For major elements analysis, ca 20 mg of sediment and rock samples were weighted in platinum crucible and digested by alkaline fusion with lithium metaborate followed by dissolution in 2 M HCl.

Major geochemical carriers (Al, Fe, Mn) were analyzed using ICP-OES (ICP Spectro Ciros Vision, Spectro). Multi-element standard solutions (Merck®) were used to produce external calibration curves. Certified reference materials (BHVO-2 and BCR-2 basalts from USGS and 1646a estuarine sediment) and an internal basalt

standard were used to assess the accuracy of analysis. The accuracy expressed as percentage relative error were always within 10% of the certified values for all the elements studied.

3.3. Zinc isotope ratio analysis

Prior to the mass spectrometry, Zn was separated from matrix components by anion exchange chromatography (Araújo et al., 2016). Bio-Rad PolyPrep columns were filled with 2 ml of the anion exchange resin AG-MP1 (100-200 mesh size) and 2 to 4 µg of zinc were loaded in 2 M HCl. Once the sample is loaded, matrix elements are eluted with 20 ml of 2 M HCl. Then zinc is eluted with 12 ml of 0.5 M HNO_3. The purified zinc fractions were evaporated to dryness and re-dissolved in 0.05 M HNO_3. To test for the complete recovery aliquots of zinc purified samples were measured by ICP-MS. The yield was 99±7%. The blanks from digestion and chromatography were less than 10 and 15 ng, respectively. The total procedural blanks were below 40 ng, which represents less than 1% of zinc content of samples.

Zinc isotope ratios were measured using the ThermoFinnigan Neptune MC-ICP-MS at the Laboratório de Geocronologia of the University of Brasília and at the Laboratorio de Geocronologia of the University of Sao Paulo. The introduction interface consisted of quartz glass spray chamber (cyclone + standard Scott double pass) coupled with a low flow PFA nebulizer (50 µl min^{-1}). After a minimum of two hours of warm up and tuning to achieve the best sensibility, the analytical sequences ran automatically using a Cetac ASX-100 autosampler and low mass resolution collector slits. Masses 62 (Ni), 63 (Cu), 64 (Zn/Ni), 65 (Cu), 66 (Zn), 67 (Zn) and 68 (Zn) were detected simultaneously. A copper standard (NIST 976) was added to all samples and matched in the proportion 1:1 (300 µg/ml in 0.05 M HNO_3).

The zinc isotopes ratios were measured relative to the in-house single element standard MERCK Lot #9953 labeled henceforward as Zn_{UnB} standard. The standard-sample bracketing technique was used, i.e, each sample was bracketed by standard solution mixture (Zn_{UnB} and $Cu_{NIST-976}$) with rinses between sample and standard analyses with 3 % (v/v) HNO_3. Instrument blanks were analyzed after each sample and each bracketing standard and on-line subtracted. Typical sample and standard signals were 3 V to ^{64}Zn and ^{65}Cu masses. Blank measurements consisted of 1 block of 10 cycles (8s) while samples and standards were measured in 2 blocks of 20 cycles of 8s each. For a single measurement (40 cycles), internal precision ranged from 3 to 8 ppm

(2σ). The raw ratios were corrected for instrumental mass fractionation using the exponential law based and the certified ratio (0.4456) for Cu of the NIST SRM 976 standard.

3.4. Zinc isotopic data presentation, reproducibility and accuracy

The δ^{66}Zn was calculated as the deviation of the mass bias corrected isotope ratio of the samples from the mean of the mass bias-corrected isotopes ratios of the bracketing standards:

$$\delta^{66}Zn(\text{‰}) = \left(\frac{^{66}Zn/ \ ^{64}Zn_{sample}}{^{66}Zn/ \ ^{64}Zn_{standard}} - 1 \right) \quad \text{eq.1}$$

Zinc isotopic data reported in this study are expressed relative to the Johnson Matthey Company 3-0749-L (JMC$_{3-0749-L}$) reference standard calibrated against our Zn$_{UnB}$ standard (ΔZn$_{JMC-UnB}$ = +0.17 ‰). Error propagations were used to calculate the error (expressed as 2σ) of δ^{66}Zn$_{JMC}$ values. The calibration is based in a total of n=30 analysis (±0.05, 2σ).

Accuracy and reproducibility of the isotope ratio determination over the study period was assessed by measuring a Zn IRMM 3702 solution two or three times during an analytical session yielding an overall δ^{66}Zn$_{JMC}$ value of -0.27 ± 0.06 ‰ (n=30, 2σ), comparable to values published previously (Moeller et al., 2012). Certified reference materials were prepared in replicates (full protocol including digestion, ion-exchange chromatography and replicated isotopic analyses) to assess procedural accuracy including the basalts BHVO-2 and BCR-2 (n=5), and the estuarine sediment NIST 1646a (n= 2). The andesite AGV-2 was prepared in a single replicate (n=1). The δ^{66}Zn$_{JMC}$ values obtained for BHVO-2 and BCR-2 were +0.25 ± 0.10‰ (2σ) and +0.25 ±0.08‰ (2σ) respectively. The δ^{66}Zn$_{JMC}$ value obtained for AGV-2 was +0.29 ±007 (2σ). These results agree well with reported in the literature (Archer and Vance, 2004; Chapman et al., 2006; Sonke et al., 2008; Moynier et al., 2010; Chen et al., 2013). The δ^{66}Zn$_{JMC}$ value for NIST 1646a was +0.32 ±0.07‰, 2σ, n=8), close to values typically found for silicate rocks and marine sediments (+0.23 ± 0.08‰, 2σ, n=20 Maréchal et al., 2000) and for sapropels (+0.28 ± 0.02‰, 2σ, n=3, Maréchal et al., 2000). Average reproducibility of certified reference materials Zn IRMM and unknown samples was

0.06‰ (2σ). This value is quoted as external reproducibility of the method and applied to all samples in all tables and graphs of this work.

4. Results

4.1 Zinc isotopic compositions and enrichment factors of sediment cores

Zinc concentrations, zinc enrichment factors (EF) and $\delta^{66}Zn_{JMC}$ values of the sediment cores are shown in Table 1 and Fig. 2. The Al-normalized EF was used to avoid dilution effects related to grain size and mineralogical heterogeneities (e.g., Salomons and Förstner, 1984) on the estimates of anthropogenic zinc inputs. It was calculated normalizing the ratio Zn/Al of samples against the corresponding ratio of granite rocks collected near the Sepetiba bay.

The $\delta^{66}Zn_{JMC}$ values of sediment cores varied from +0.30 to +1.15‰. Core T1, sampled within the mangrove of the Saco do Engenho creek, the *hot spot* of electroplating waste contamination, showed the heaviest $\delta^{66}Zn_{JMC}$ values, ranging between +0.72 to +1.15‰. Zinc concentrations were extremely elevated (up to 4% sediment dry weight) and Zn EF values ranged between 117 and 784. From the core base to the 40 cm depth, the isotopic signatures changed toward lighter values, reaching +0.72‰. From 40 cm depth to upper layers, the isotopic signatures also show large variations, with peaks of +1.03 and +1.00‰ at 25 and 10 cm depth, respectively. Core T2 located near to the Saco do Engenho creek mouth, has also very high Zn EF, varying between 68 to 697, and heavier isotopic compositions, though with a smaller range of $\delta^{66}Zn_{JMC}$ values (+0.65 to +0.83‰) than core T1. A slight upward shift to heavier isotopic composition occurs in this core, although most isotopic signatures are statistically not differentiable (taking the error bars into account, ±0.06‰). Core T3 (São Francisco channel mouth) displays Zn EF values between 1.7 to 8.2 and the $\delta^{66}Zn_{JMC}$ values range between +0.30 and +0.75‰. This profile shows a progressive increase of $\delta^{66}Zn_{JMC}$ values and Zn EF from bottom to the middle, with a salient peak at 20 cm depth corresponding to the heaviest $\delta^{66}Zn_{JMC}$ value (+0.75‰) and highest Zn EF value (8.2). Following this peak, $\delta^{66}Zn_{JMC}$ and Zn EF values decrease to +0.46‰ and 3.8 in the core top. Core T4 (Enseada das Garças) displays higher Zn EF than T3 core (ranging between 11.9 and 18.2). The $\delta^{66}Zn_{JMC}$ values from this core show isotopically heavy zinc (+0.67 to +0.74‰), comparable to T1 and T2 cores collected near the old wastes of the metallurgical refining. From the base to the top, $\delta^{66}Zn_{JMC}$ and Zn EF values decrease slightly (Fig.2). Core T5 (Marambaia) shows $\delta^{66}Zn_{JMC}$ values

comparable to core T3. From the base (45 cm) to 35 cm depth, Zn EF and δ^{66}Zn values increase from 10.5 and +0.60‰ to 14.2 and +0.71‰, respectively. Above 35 cm depth, Zn EF and δ^{66}Zn values decreased continuously until the values of 6.9 and +0.36‰, respectively (Fig.2).

4.2 Zinc isotope compositions of SPM, rocks and ores

The results for the SPM are presented in the Table 2. The samples collected close to the mouth of Saco do Engenho channel show δ^{66}Zn$_{JMC}$ values ranging from +0.83 to +0.88‰ and high average Zn concentrations of 1,242 ± 198 µg g^{-1} (1σ, n= 3). The SPM from the rivers show an average concentrations of 99 ± 13 µg.g^{-1} (1σ, n= 2) and isotope signatures of +0.27 ±0.11‰ (2σ, n= 3). The SPM samples collected at the west side of the bay, being strongly influenced by the marine source (B1, B2, B3 samples), display δ^{66}Zn$_{JMC}$ values around +0.45 ±0.03‰ (2σ, n= 3) and low zinc concentrations ranging around 45 ±3 µg.g^{-1} (1σ, n= 3). The granites have average δ^{66}Zn$_{JMC}$ value of +0.21 ± 0.01‰ (2σ, n= 2), while willemite ores have δ^{66}Zn$_{JMC}$ values ranging between -0.1 and +0.14‰ (average of 0.03 ± 0.24‰, n= 3) (Table 1).

4.3 Major geochemical carriers profiles

The concentrations of the major elements Al, Fe and Mn, and Fe/Mn ratios are shown in Table 1. The profiles of Fe/Mn ratios are shown in Fig.3. These rations were included to constrain possible redox processes, since these metals present different mobility in response to redox gradients. Under reducing conditions, while manganese tend to be more remobilized, iron tend to remain retained in the solid phase as stable iron sulfides (Burdige, 1993; Maynard, 2003). The cycling of Mn and Fe influence the diffusion of dissolved trace elements across the sediment–water interface and the remobilization and repartitioning along redox gradients within the sediments (Shaw et al., 1990; Tribovillard et al., 2006).

The core T1, collected in the mangrove of Saco do Engenho, shows the highest average values (1.3 ± 0.72) and the largest variations for Fe/Mn ratios (from 0.57 to 3.21), with positive peaks at 15 and 40 cm depth. The ratios along the profiles of mud flat cores were lower than 1.4 for T2 and T3 cores and 0.9 for T4 and T5 cores. The profiles also are less variable, generally with major changes in the first 10 cm from the top (Fig.3).

11

5. Discussion

5.1 Identifying sources, pathways and sinks of zinc in the coastal system using the stable isotope composition

The chemical composition of the sediments at Sepetiba bay is controlled by the mixture of continental, marine, autochthonous and anthropogenic materials (Barcellos et al., 1997). The zinc isotopic signatures of sediment cores and SPM samples indicate that contributions of these major sources varied spatially and temporally (Fig.2). The SPM collected in the fluvial system of São Francisco channel and Gandu river represent the continental material brought to the bay, showing $\delta^{66}Zn_{JMC}$ values of +0.27 ±0.11‰ (2σ) (Fig.4A). It is suspected that these materials encompass natural terrigenous zinc mixed with anthropogenic zinc derived of industrial and urban diffuse sources from the bay watershed. However, the low zinc concentrations of R1 and R2 samples (90 and 108 μg g^{-1}, respectively; Table 2), similar to pre-industrial values derived from dated Sepetiba Bay sediments (69 to 103 μg g^{-1}; Marques et al., 2006), suggest a large dominance of natural terrigenous materials. The oceanic detrital material that enters the bay from the west is characterized by $\delta^{66}Zn_{JMC}$ values of +0.45 ±0.03‰ (2σ). These $\delta^{66}Zn_{JMC}$ values are slightly above the range of +0.2 to +0.4‰ commonly reported for silicate rocks (Fig.4A; Cloquet et al., 2007; Chen et al.2013). However, cases of geological settings with heavier $\delta^{66}Zn$ values have been reported (e.g., Taiwan orogen; Bentahila et al., 2004). This oceanic material may be associated to weathered rocks of adjacent coastal zones.

The highly contaminated T1 and T2 cores, located within the old metallurgic zone, have $\delta^{66}Zn_{JMC}$ values ranging from +0.68 to +1.15‰, which are similar to those reported for wastes and slags of metallurgy industry, ranging from +0.59 to +1.49‰ (Fig.4A). Based on these impacted sediments, we calculate an average of $\delta^{66}Zn_{JMC}$ values of +0.86 ±0.15‰ as the best estimate for the isotopic signature of the original electroplating wastes. These isotopic signatures indicate a large fractionation factor induced by high temperature processes employed during the roasting step in the electroplating plant. According to Rayleigh's law, lighter zinc isotopes enter the vapor phase leaving the residual material (e.g., fly ash particles and slags) enriched with the heavier isotopes (Sivry et al., 2008; Borrok et al., 2010; Yin et al., 2015; Gonzalez and Weiss, 2016). In the case of ores refining, the additional electroplating step seems also to affect the zinc isotope fractionation, as demonstrated in controlled electrochemical

12

experiments (Kavner et al.,2008, Black et al., 2011; Black et al., 2014). The exact contribution of roasting and electroplating steps on the overall zinc isotope fractionation of ores and wastes is difficult to determine.

As expected, the SPM collected near the mouth of Saco do Engenho creek displayed an average $\delta^{66}Zn_{JMC}$ value similar to T1 and T2 cores, i.e. +0.84 ±0.07‰, 2σ (Fig.4A). The SPM dispersion is controlled by tides and surface currents and tends to be deposited in the mud and tidal flats and mangroves forests along the northeastern coastal area of the bay (Lacerda et al., 1988; Roncarati and Carelli, 2012; Montezuma, 2013). In the tidal flat area, represented by T4 core, $\delta^{66}Zn_{JMC}$ values were about +0.67 to +0.74‰, and therefore, comparable to the heavy isotopic signatures of T1 and T2 cores and SPM samples from the Saco do Engenho (Fig.4A). In the mud flat located in the southeastern bay, the core T5 shows lighter $\delta^{66}Zn_{JMC}$ values and lower Zn concentrations than T1, T2 and T4 cores, but also shows evidence of a strong influence of anthropogenic zinc coming from the electroplating wastes (Fig. 4A). All these results clearly show that the anthropogenic zinc derived from this source is dispersed in the inner bay and dominate over the continental and oceanic sources in the mud and tidal flat areas.

In the mud flat close the São Francisco Channel, the core T3 has $\delta^{66}Zn_{JMC}$ values encompassing those found in granite rocks samples and in old electroplating wastes (Fig. 4A). The base of the T3 core (i.e., 45-55 cm depth) has low zinc concentrations (105 to 111 μg g^{-1}) that likely represent deposition from the pre-industrial period (Marques et al., 2006), with $\delta^{66}Zn_{JMC}$ signatures (+0.30 to +0.33‰) close to those from SPM sampled at stations R1 and R2 (+0.27±0.11‰). The average $\delta^{66}Zn_{JMC}$ value for granite rock and the base profile samples of T3 core have a value of +0.28 ±0.12‰ (2σ, n= 3). This value is considered the best estimate of the local terrestrial background source.

The relationship between zinc isotope compositions and concentrations of sediments indicate a mixing source process. Using enrichment factors values rather than zinc concentrations, the mixing trends become more noticeable with strong positive correlation with $\delta^{66}Zn$ and Zn EF values in cores T2, T3, T4 and T5 (R^2= 0.90, 0.87, 0.84 and 0.74, p < 0.01, respectively; Fig. 4B).

The mud flat results indicate that anthropogenic zinc isotopic signatures remain nearly unaltered during transport associated to SPM and by post depositional processes. The Fe/Mn ratios in the mud flat cores (T2, T3, T4, T5 cores; Fig. 2) suggest moderate

variations of redox processes (e.g., triggered by bioturbation), suggesting a relatively low potential to affect the geochemical records of trace metals. The ^{210}Pb profiles of dated sediments of Sepetiba bay and their consistence with temporal changes of zinc and cadmium concentrations during the beginning of industrialization and metallurgic impacts of the bay, are additional evidences of geochemical records preservation in the mud flats (Molisani et al., 2004; Marques et al., 2006; Gomes et al., 2009; Patchineelam et al., 2011). Moreover, the sediment pool account for more than 99% of total zinc budget (Lacerda et al., 1987; Costa et al., 2005) and a simple mass balance between the sediment and dissolved phase suggest that biogeochemical processes typically operating in this estuary probably are not enough to change the isotope compositions of zinc in the sediments.

In the mangrove core (T1), differing from mud flat cores, the δ^{66}Zn values and Zn EF (Fig. 4B) are not significantly correlated. Moreover, it presents some outliers with heavier δ^{66}Zn values in the base of the profile (1.09 and 1.15‰ at the 75-80 and 80-85 cm depth intervals). This core shows larger variations in the Zn EF and Fe/Mn values (Fig. 2 and Fig.3), which suggest possible remobilization of zinc within the sediments due to redox processes. Mangrove sediments can develop these gradients due to tidal water oscillations, diagenesis, rhizosphere reactions (e.g., O_2 inputs by the roots) and bioturbation (Clark et al., 1998; Marchand et al., 2006; Machado et al., 2014). In turn, zinc remobilization and significant changes in the Zn isotopic record in sediments due to plant uptake are not expected, since mangrove vegetation show low bioaccumulation of metals (Marchand et al., 2006; Lewis et al., 2011). In Sepetiba bay, *Rhizophora mangle* (red mangrove) biomass contain less than 1% of zinc compared to sedimentary reservoir (Silva et al., 1990).

This impacted mangrove site presents anomalously high zinc concentrations (from 0.5% to 4%) and a high load of zinc bound to labile geochemical fractions of sediments (Lacerda and Molisani, 2006), which can be partly be released to pore waters during post-depositional biogeochemical processes. Radiotracer experiments have evidenced that trace metal vertical diffusion within mangrove sediments from Sepetiba Bay is largely controlled by biological activity such as bioturbation (Suzuki et al., 2012, 2013). Thus, we suspect that zinc isotopic signatures within the mangrove sediments are more susceptible to alterations by post-depositional fractionation processes than expected for the unvegetated mud flat sediments.

We are not able to develop an isotope mechanism in the water-sediment interface due the lack of information of dissolved phase. However, we hypothesize that processes of release and immobilization of zinc (e.g., in the different Fe-minerals phases within mangrove rhizospheres; Clark et al., 1998; Marchand et al., 2006) could result in significant isotopic fractionation within mangrove sediments. During anoxic conditions (e.g, during high tides), Fe-oxyhydroxides are partially reduced and the insoluble iron and trace elements sulfides are formed, as driven by microbial activity (Huerta-Diaz and Morse, 1992; Andrade et al., 2012). In turn, insoluble sulfide phases are partly oxidized during oxic conditions (e.g, during low tides), resulting in the partial release of trace metals to pore water or in the immobilization of these elements in Fe-oxyhydroxides (Lacerda et al., 1993; Otte et al., 1995; Purnobasuki and Suzuki, 2005; Marchand et al., 2011; Zhou et al., 2011; Machado et al., 2014).

While experimental work reported zinc isotopic fractionation at the surface of iron oxides with respect to the coexisting solution, with $\Delta^{66}Zn_{solid-solution}$ of +0.29 ±0.07‰ and +0.53 ±0.07 ‰ (Balistrieri et al., 2009; Juillot et al., 2008), other studies have shown that the light isotopes likely became enriched in the sulfidic phases (John et al., 2008; Kelley et al., 2009; Veeramani et al., 2015). Therefore, it is plausible that the cycling of zinc within sedimentary mangrove environments, coupled to well-known intense redox reactions, experience significant isotopic fractionation. However, the $\delta^{66}Zn$ outlier values near the base of the profile does not limit the identification of the metallurgic zinc signature, since these heavier values slightly exceed (by less than +0.16‰) the average $\delta^{66}Zn$ value from the whole core (+0.90‰).

5.2 A mixing model for zinc

A plot of $\delta^{66}Zn$ against Zn concentrations and EF (Fig. 4A and 4B), using all available data, reveals different trends. The core T3 samples (São Francisco estuary) plot on a straight line between granite rocks and the metallurgic impacted sediments of Saco do Engenho, suggesting binary mixture between the anthropogenic and terrestrial end members, respectively (Fig.4A and 4B). However, the isotope signatures found in cores T4 and T5 (located in the southeastern and southwestern areas of the bay, respectively; Fig.1) do not aligning with granite rock isotope compositions or marine SPM (Fig.4A and 4B). This deviation may be explained by the influence of additional sources on the isotopic compositions in the region south of the bay, linked to the intense urban expansion and industrial development in the watershed of Sepetiba bay after the 1970's

(Molisani et al., 2004). The $\delta^{66}Zn_{JMC}$ values of the most common urban anthropogenic sources tend to be lower than the average of silicate rocks (+0.28 ±0.05‰, Chen et al., 2013), such as tire wear (+0.04 ±0.2‰, Thapalia et al., 2010), vehicle emission (-0.87 to +0.07, Gioia et al., 2008), urban runoff (from +0.13 to +0.15‰, Chen et al., 2009) and wastewaters and sludge (~0.1‰; Chen et al., 2009). These source differences may explain the lighter isotopic signatures in the T4 and T5 cores in comparison with T3 core for similar EF values (Fig.4B).

In this way, we suggest that zinc isotopic signatures of sediments in the northeastern area of the bay are derived from binary mixing of metallurgic and natural terrestrial sources, while sediments in the southern areas of the bay are influence by a third endmember, associated to diffuse contamination from industrial and urban sources.

Despite some deviations, the isotopic signatures of most samples are dominated by the terrestrial background and the major anthropogenic zinc source (Fig.4A e 4B). This allows the application of a simple binary mixture model to quantify the relative contribution from the major anthropogenic Zn source ($Zn_{anth.\%}$), according to the equation below:

$$Zn_{anthr.\%} = \left(\frac{\delta_{sample} - \delta_{terrestrial}}{\delta_{anthropogenic} - \delta_{terrestrial}} \right) * 100 \quad \text{eq.2,}$$

The Fig.5 shows the $Zn_{anth.\%}$ estimated for cores T3, T4 and T5. Since cores T1 and T2 represent the isotopic composition essentially from the anthropogenic end member, they were not considered in the mixing model. We find a clear evolution from a period without significant contribution from electroplating wastes discharge into the bay (with low $Zn_{anth.\%}$ values at the base of profile; < 10%) to periods of dominant contributions from this source were observed in the profile T3. In core T4, however, only high contributions from the major anthropogenic Zn source were found ($Zn_{anth.\%} \geq 70\%$), which suggests that only the post-industrialization period was recorded. In the core T5, the $Zn_{anth.\%}$ varied high values at deeper layers (between 50% and 70% below 35 cm depth) and a tendency of decreasing above 25 cm depth, reaching the lowest $Zn_{anth.\%}$ value of 14%. As diffuse sources may have contributed for the accumulation of zinc, which would lead to lighter isotope compositions than that from the electroplating waste

16

endmember, it is important to note that the percentage of anthropogenic zinc related to electroplating wastes may be minimal estimates.

Previous work using dated cores from Sepetiba Bay confirmed that the significant changes in zinc concentrations in the cores relate to the beginning of the electroplating plant in the 1960 (Molisani et al., 2004; Marques et al., 2006; Gomes et al., 2009; Patchineelam et al., 2011). The $Zn_{anth.\%}$ peaks found in the core T3 and T5 corroborate these previous observations, as attested by the isotopic source signature assessment. Another important feature of cores T3 and T5 is that the observed Zn EF in uppermost layers (Fig.2) is associated to a smaller contribution from major industrial source. While the wastes removal tends to attenuate the Zn electroplating contamination in the bay, an increase in the relative importance of other anthropogenic sources may occur (Molisani et al., 2004). Therefore, further characterization of diffuse sources contributions to determine the Zn loading to the bay will be useful for monitoring input of these zinc sources to the bay. This Zn isotopic model could benefit coastal areas worldwide with analogous contexts of Zn contamination.

6. Conclusions

The zinc isotopic compositions of sediment samples and SPM collected in the Sepetiba Bay, Rio de Janeiro, Brazil, and of willemite ores, show significant variation of $\delta^{66}Zn_{JMC}$ values (-0.01 to +1.15‰). The main conclusions derived from these results are:

1. The Zn isotope composition of sediments are well explained by a mixing model, including three sources, i.e. terrestrial background (+0.28 ± 0.12‰, 2σ), marine (+0.45 ±0.03‰, 2σ) and the major anthropogenic (+086±0.15‰, 2σ) endmembers, this last corresponding to electroplating wastes. Additional sources such as diffuse pollution associated to sewage and other industrial effluents are suspected and require future investigations.

2. The sediment cores collected in the mud flat of the bay show good correlation between $\delta^{66}Zn$ values and Zn enrichment factors, indicating that the source record is well preserved in the sediments.

3. It is suspected that the isotopic signature of the electroplating wastes in the mangrove core is slightly modified at some layers due to biogeochemical processes triggered by tidal cycles, bioturbation and rhizospheres. However, these processes do not compromise the isotopic identification of the anthropogenic Zn source.

4. Negligible contributions of marine sources and the dominance of terrestrial and major anthropogenic sources in the inner bay, allowed the application of a binary mixing model to quantify relative contributions from these sources. The calculations suggest contributions of anthropogenic Zn ranging from negligible values, during the pre-industrial period, up to 80% during the industrial period. The relative contribution of the major anthropogenic source of Zn has decreased in some specific regions of the bay, after the end of metallurgical activities in 1998.

5. Zinc isotopes successfully trace spatial and temporal variations in source contributions of metallurgical wastes in a complex ecosystem such as a coastal area, confirming previous finding that Zn isotopes are an effecting tracer of anthropogenic sources in the environment, and therefore, can be useful to support prevention and monitoring in coastal sites.

References

Abrahim G. and Parker R. (2007) Assessment of heavy metal enrichment factors and the degree of contamination in marine sediments from Tamaki Estuary, Auckland, New Zealand. *Environ.Monit. Assess.***136**, 227-238.

Adriano D. and Adriano D. (2001) *Trace elements in terrestrial environments*. Springer, New York.

Alves R., Sampaio C., Nadal M., Schuhmacher M., Domingo J. and Segura-Muñoz S. (2014) Metal concentrations in surface water and sediments from Pardo River, Brazil: Human health risks. *Environ. Rese.***133**, 149-155.

Amado Filho G., Andrade L., Karez C., Farina M. and Pfeiffer W. (1999) Brown algae species as

biomonitors of Zn and Cd at Sepetiba Bay, Rio de Janeiro, Brazil. *Mar. Environ. Res*. **48**, 213-224.

Andrade R., Sanders C., Boaventura G. and Patchineelam S. (2012) Pyritization of trace metals in mangrove sediments. *Environ. Earth. Sci.* **67**, 1757-1762.

Araújo D., Boaventura G., Viers J., Mulholland D., Weiss D., Araújo D., Lima B., Ruiz I., Machado W., Babinski M. and Dantas E. (2016) Ion Exchange Chromatography and Mass Bias Correction for Accurate and Precise Zn Isotope Ratio Measurements in Environmental Reference Materials by MC-ICP-MS. *J. Brazil. Chem. Soc*. DOI: 10.5935/0103-5053.20160167.

Archer C. and Vance D. (2004) Mass discrimination correction in multiple-collector plasma source mass spectrometry: an example using Cu and Zn isotopes. *J. Anal. Atom. Spectrom.* **19**, 656.

Balistrieri L., Borrok D., Wanty R. and Ridley W. (2008) Fractionation of Cu and Zn isotopes during adsorption onto amorphous Fe(III) oxyhydroxide: Experimental mixing of acid rock drainage and ambient river water. *Geochim. Cosmochim. Ac.* **72**, 311-328.

Barcellos C. and Lacerda L. (1994) Cadmium and zinc source assessment in the Sepetiba Bay and basin region. *Environm. Monit. Assess.* **29**, 183-199.

Barcellos C., Lacerda L. and Ceradini S. (1997) Sediment origin and budget in Sepetiba Bay (Brazil) - an approach based on multielemental analysis. *Environm. Geol.* **32**, 203-209.

Barone R.H.T.(1973) Perfil analítico do zinco. Ministério das Minas e Energia. Departamento Nacional da Produçao Mineral. Bolteim nº26. Rio de Janeiro, Brasil.

Bastami K., Neyestani M., Shemirani F., Soltani F., Haghparast S. and Akbari A. (2015) Heavy metal pollution assessment in relation to sediment properties in the coastal sediments of the southern Caspian Sea. *Mar. Poll. Bull.* **92**, 237-243.

Bhardwaj V., Singh D. and Singh A. (2009) Environmental repercussions of cane-sugar industries on the Chhoti Gandak river basin, Ganga Plain, India. *Environ. Monit. Asses.* **171**, 321-344.

Bianchi T. (2007) *Biogeochemistry of estuaries*.Oxford University Press, Oxford.

Borrok D., Gieré R., Ren M. and Landa E. (2010) Zinc Isotopic Composition of Particulate Matter Generated during the Combustion of Coal and Coal + Tire-Derived Fuels. *Environ. Sci. Tech.* **44**, 9219-9224.

Burdige D. (1993) The biogeochemistry of manganese and iron reduction in marine sediments. *Earth Sci. Rev.* **35**, 249-284.

Chen H., Savage P., Teng F., Helz R. and Moynier F. (2013) Zinc isotope fractionation during magmatic differentiation and the isotopic composition of the bulk Earth. *Earth Planet. Sci. Letters.* **369-370**, 34-42.

Chen J., Gaillardet J. and Louvat P. (2008) Zinc Isotopes in the Seine River Waters, France: A Probe of Anthropogenic Contamination. *Environ. Sci. Technol.* **42**, 6494-6501.

Chen J., Gaillardet J., Louvat P. and Huon S. (2009) Zn isotopes in the suspended load of the Seine River, France: Isotopic variations and source determination. *Geochim. Cosmochim. Ac.* **73**, 4060-4076.

Clark J. (1996) *Coastal zone management handbook*. CRC Press, Boca Raton, Fla.

Clark M., McConchie D., Lewis D. and Saenger P. (1998) Redox stratification and heavy metal partitioning in Avicennia-dominated mangrove sediments: a geochemical model. *Chem. Geol.* **149**, 147-171.

Cloquet C., Carignan J., Lehmann M. and Vanhaecke F. (2007) Variation in the isotopic composition of zinc in the natural environment and the use of zinc isotopes in biogeosciences: a review. *Anal. Bioanal. Chem.* **390**, 451-463.

Costa A., Anjos M., Lopes R., Pérez C. and Castro C. (2005) Multi-element analysis of sea water from Sepetiba Bay, Brazil, by total reflection x-ray fluorescence spectrometry using synchrotron radiation. *X-Ray Spectrom.* **34**, 183-188.

Dolgopolova A., Weiss D., Seltmann R., Kober B., Mason T., Coles B. and Stanley C. (2006) Use of isotope ratios to assess sources of Pb and Zn dispersed in the environment during mining and ore processing within the Orlovka–Spokoinoe mining site (Russia). *Appl. Geochem.* **21**, 563-579.

Du Laing G., Rinklebe J., Vandecasteele B., Meers E. and Tack F. (2009) Trace metal behaviour in estuarine and riverine floodplain soils and sediments: A review. *Sc. Total Environ* **407**, 3972-3985.

Gioia S., Weiss D., Coles B., Arnold T. and Babinski M. (2008) Accurate and Precise Zinc Isotope Ratio Measurements in Urban Aerosols. *Anal. Chem.* **80**, 9776-9780.

Gomes F. de C., Godoy J., Godoy M., Lara de Carvalho Z., Tadeu Lopes R., Sanchez-Cabeza J., Drude de Lacerda L. and Cesar Wasserman J. (2009) Metal concentrations, fluxes, inventories and chronologies in sediments from Sepetiba and Ribeira Bays: A comparative study. *Mar. Pollut. Bull.* **59**, 123-133.

Gordon R., Graedel T., Bertram M., Fuse K., Lifset R., Rechberger H. and Spatari S. (2003) The characterization of technological zinc cycles. *Res. Conserv. Rec.* **39**, 107-135.

Hudson-Edwards K., Jamieson H. and Lottermoser B. (2011) Mine Wastes: Past, Present, Future.

Elements **7**, 375-380.

Huerta-Diaz M. and Morse J. (1992) Pyritization of trace metals in anoxic marine sediments. *Geochim. Cosmochim. Ac.* 56, 2681-2702.

John S., Genevieve Park J., Zhang Z. and Boyle E. (2007) The isotopic composition of some common forms of anthropogenic zinc. *Chem. Geol.* **245**, 61-69.

John S., Rouxel O., Craddock P., Engwall A. and Boyle E. (2008) Zinc stable isotopes in seafloor hydrothermal vent fluids and chimneys. *Earth Planet. Sci. Lett.* **269**, 17-28.

Kasuya M., Teranishi H., Aoshima K., Katoh T., Horigushi H., Morikawa Y., Nishijo M. and Iwata, K. (1992) Water pollution by cadmium and the onset of Itai-itai disease. *Water Sci. Technol.* **25**, 149-156.

Kavner A., John S., Sass S. and Boyle E. (2008) Redox-driven stable isotope fractionation in transition metals: Application to Zn electroplating. *Geochim. Cosmochim. Ac.* **72**, 1731-1741.

Kelley K., Wilkinson J., Chapman J., Crowther H. and Weiss D. (2009) Zinc isotopes in sphalerite from base metal deposits in the red dog district, northern Alaska. *Econ. Geol.* **104**, 767-773.

Kim B., Salaroli A., Ferreira P., Sartoretto J., Mahiques M. and Figueira R. (2016) Spatial distribution and enrichment assessment of heavy metals in surface sediments from Baixada Santista, Southeastern Brazil. *Mar. Poll. Bull.* **103**, 333-338.

Kunzmann M., Halverson G., Sossi P., Raub T., Payne J. and Kirby J. (2012) Zn isotope evidence for immediate resumption of primary productivity after snowball Earth. *Geology* **41**, 27-30.

Lacerda L., Carvalho C., Tanizaki K., Ovalle A. and Rezende C. (1993) The Biogeochemistry and Trace Metals Distribution of Mangrove Rhizospheres. *Biotropica* **25**, 252.

Lacerda L., Martinelli L., Rezende C., Mozeto A., Ovalle A., Victoria R., Silva C. and Nogueira F. (1988) The fate of trace metals in suspended matter in a mangrove creek during a tidal cycle. *Sci. Total Environ.* **75**, 169-180.

Lacerda L. and Molisani M. (2006) Three decades of Cd and Zn contamination in Sepetiba Bay, SE Brazil: Evidence from the mangrove oyster Crassostraea rhizophorae. *Mar. Pollut. Bull.* **52**, 974-977.

Lacerda L., Pfeiffer W. and Fiszman M. (1987) Heavy metal distribution, availability and fate in Sepetiba Bay, S.E. Brazil. *Sci. Total Environ.* **65**, 163-173.

Langston W. and Bebianno M. (1998) *Metal metabolism in aquatic environments*. Chapman & Hall, London.

Leal Neto A., Legey L., González-Araya M. and Jablonski S. (2006) A System Dynamics Model for the Environmental Management of the Sepetiba Bay Watershed, Brazil. *Environ. Manage.* **38**, 879-888.

Lewis M., Pryor R. and Wilking L. (2011) Fate and effects of anthropogenic chemicals in mangrove ecosystems: A review. *Environ. Pollut.* **159**, 2328-2346.

Machado W., Borrelli N., Ferreira T., Marques A., Osterrieth M. and Guizan C. (2014) Trace metal pyritization variability in response to mangrove soil aerobic and anaerobic oxidation processes. *Mar. Pollut. Bull.* **79**, 365-370.

Marchand C., Allenbach M. and Lallier-Vergès E. (2011) Relationships between heavy metals distribution and organic matter cycling in mangrove sediments (Conception Bay, New Caledonia). *Geoderma* **160**, 444-456.

Marchand C., Lallier-Vergès E., Baltzer F., Albéric P., Cossa D. and Baillif P. (2006) Heavy metals distribution in mangrove sediments along the mobile coastline of French Guiana. *Mar. Chem.* **98**, 1-17.

Marcovecchio J., Botté S. and Fernández Severini M. (2016) Distribution and behavior of zinc in estuarine environments: an overview on Bahía Blanca estuary (Argentina). *Environ Earth Sci* **75**.

Maréchal C., Nicolas E., Douchet C. and Albarède F. (2000) Abundance of zinc isotopes as a marine biogeochemical tracer. *Geochem. Geophy. Geosystems* **1**, (5).

Marques A.N., Monna F., da Silva Filho E., Fernex F. and Fernando Lamego Simão Filho F. (2006) Apparent discrepancy in contamination history of a sub-tropical estuary evaluated through ^{210}Pb profile and chronostratigraphical markers. *Mar. Pollut. Bull.* **52**, 532-539.

Mason R.(2013) *Trace metals in aquatic systems*. Willey-Blackwell, Oxford.

Mason T., Weiss D., Chapman J., Wilkinson J., Tessalina S., Spiro B., Horstwood M., Spratt J. and Coles B. (2005) Zn and Cu isotopic variability in the Alexandrinka volcanic-hosted massive sulphide (VHMS) ore deposit, Urals, Russia. *Chem. Geol.* **221**, 170-187.

Mattielli N., Rimetz J., Petit J., Perdrix E., Deboudt K., Flament P. and Weis D. (2006) Zn-Cu isotopic study and speciation of airborne metal particles within a 5-km zone of a lead/zinc smelter. *Geochim. Cosmochim. Ac.* **70**, A401.

Moeller K., Schoenberg R., Pedersen R., Weiss D. and Dong S. (2012) Calibration of the New Certified

Reference Materials ERM-AE633 and ERM-AE647 for Copper and IRMM-3702 for Zinc Isotope Amount Ratio Determinations. *Geostandards Geoanal.Res.* **36**, 177-199.

Molisani M.M., Marins R.V., Machado W., Paraquetti H.H.M., Bidone E.D., and Lacerda L.D. (2004) Environmental changes in Sepetiba Bay, SE Brazil. *Reg. Environ. Change* **4**, 17-27.

Montezuma P.N. (2012) Análise de prováveis fatores causadores do processo de assoreamento na Baía de Sepetiba-RJ. In: *Bacia hidrográfica dos Rios Guandu, da Guarda e Guandu-Mirim*. INEA, Rio de Janeiro.

Ochoa Gonzalez R., Strekopytov S., Amato F., Querol X., Reche C. and Weiss D. (2016) New Insights from Zinc and Copper Isotopic Compositions into the Sources of Atmospheric Particulate Matter from Two Major European Cities. *Environ. Sci. Technol.* **50**, 9816-9824.

Ochoa Gonzalez. R. and Weiss D. (2015) Zinc Isotope Variability in Three Coal-Fired Power Plants: A Predictive Model for Determining Isotopic Fractionation during Combustion. *Environ. Sci. Technol.* **49**, 12560-12567.

Otte M., Kearns C. and Doyle M. (1995) Accumulation of arsenic and zinc in the rhizosphere of wetland plants. *Bull. Environ. Contam. Toxicol. 55,* 154– 161

Pan K. and Wang W. (2012) Trace metal contamination in estuarine and coastal environments in China. *Sci. Total Environ..* **421-422**, 3-16.

Patchineelam S., Sanders C., Smoak J., Zem R., Oliveira G. and Patchineelam S. (2011) A historical evaluation of anthropogenic impact in coastal ecosystems by geochemical signatures. *J. Braz. Chem. Soc.* **22**, 120-125.

Pellegatti F., Figueiredo A. and Wasserman J. (2001) Neutron Activation Analysis Applied to the Determination of Heavy Metals and Other Trace Elements in Sediments from Sepetiba Bay (RJ), Brazil. *Geostand. Geoanal. Rese.* **25**, 307-315.

Petit J., Schäfer J., Coynel A., Blanc G., Chiffoleau J., Auger D., Bossy C., Derriennic H., Mikolaczyk M., Dutruch L. and Mattielli N. (2015) The estuarine geochemical reactivity of Zn isotopes and its relevance for the biomonitoring of anthropogenic Zn and Cd contaminations from metallurgical activities: Example of the Gironde fluvial-estuarine system, France. *Geochim. Cosmochim. Ac.* **170**, 108-125.

Pichat S., Douchet C. and Albarède F. (2003) Zinc isotope variations in deep-sea carbonates from the eastern equatorial Pacific over the last 175 ka. *Earth Planet. Sci.Lett.* **210**, 167-178.

Purnobasuki H. and Suzuki M. (2005) Functional Anatomy of Air Conducting Network on the Pneumatophores of a Mangrove Plant, Avicennia marina (Forsk.) Vierh. *Asian J. Plant Sci.* **4**, 334-347.

Rebelo M., Clara Rebouças do Amaral M. and Chritstian Pfeiffer W. (2003) High Zn and Cd accumulation in the oyster Crassostrea rhizophorae, and its relevance as a sentinel species. *Mar. Pollut. Bull.* **46**, 1354-1358.

Rodrigues M.A.C.; Silvia D.P and Santos S.B. dos.(2012) *Baía de Sepetiba: Estado da Arte*. Rio de Janeiro. Corbã.

Roncarati H., and Carelli S.G. (2012) Consideraçoes sobre estado da arte dos processos geológicos cenozóicos atuantes na baía de Sepeitba. In *Baía de Sepetiba: Estado da Arte* (ed. M.A.C Rodrigues, S.D Pereira, S.B dos Santos).Corbã, Rio de Janeiro. pp. 12-36.

Salomons W. and Förstner U. (1984) Metals in the Hydrocycle. Springer, Berlin.

Shaw T.J., Gieskes J.M. and Jahnke R.A. (1990) Early diagenesis in differing depositional environments: the response of transition metals in pore water. *Geochim. Cosmochim. Acta* **54**,1233-1246.

Shiel A., Weis D. and Orians K. (2010) Evaluation of zinc, cadmium and lead isotope fractionation during smelting and refining. *Sci. Total Environ.* **408**, 2357-2368.

Silva C., Lacerda L. and Rezende C. (1990) Metals Reservoir in a Red Mangrove Forest. *Biotropica* 22, 339.

Singh S., Subramanian V. and Gibbs R. (1984) Hydrous Fe and Mn oxides-scavengers of heavy metals in the aquatic environment. *Crit. Rev. Environ. Contr.* **14**, 33-90.

Sivry Y., Riotte J., Sonke J., Audry S., Schafer J., Viers J., Blanc G., Freydier R. and Dupre B. (2008) Zn isotopes as tracers of anthropogenic pollution from Zn-ore smelters The Riou Mort-Lot River system. *Chem. Geol.* **255**, 295-304.

Smoak J.M and Patchineelam S.R (1999) Sediment mixing and accumulation in a mangrove ecosystem evidence from ^{210}Pb, [234]Th and [7]Be. *Mang. Salt Marsh.* **3**:17–27

Sonke J., Sivry Y., Viers J., Freydier R., Dejonghe L., Andre L., Aggarwal J., Fontan F. and Dupre B. (2008) Historical variations in the isotopic composition of atmospheric zinc deposition from a zinc smelter. *Chem. Geol.* **252**, 145-157.

Suzuki K.N., Machado E.C., Machado W., Bellido A.V.B., Bellido L.F., Osso J.A. and Lopes R.T. (2012). Selenium, chromium and cobalt diffusion into mangrove sediments: radiotracer experiment evidence of coupled effects of bioturbation and rhizosphere. Water Air Soil Pollut. **223**, 3887-3892.

Suzuki K.N., Machado E.C., Machado W., Bellido L.F., Bellido A.V.B. and Lopes R.T. (2013). Radiotracer estimates of benthic activity effects on trace metal diffusion into mangrove sediments. Mar. Environ. Res. **83**, 96-100.

Thapalia A., Borrok D., Van Metre P., Musgrove M. and Landa E. (2010) Zn and Cu Isotopes as Tracers of Anthropogenic Contamination in a Sediment Core from an Urban Lake. *Environ. Sci Technol.* **44**, 1544-1550.

Thapalia A., Borrok D., Van Metre P. and Wilson J. (2015) Zinc Isotopic Signatures in Eight Lake Sediment Cores from Across the United States. *Environ. Sci. Technol.* **49**, 132-140.

Tribovillard N., Algeo T., Lyons T. and Riboulleau A. (2006) Trace metals as paleoredox and paleoproductivity proxies: An update. *Chemical Geology* 232, 12-32.

Turner A. (1996) Trace-metal partitioning in estuaries: importance of salinity and particle concentration. *Mar. Chem.* **54**, 27-39.

Veeramani H., Eagling J., Jamieson-Hanes J., Kong L., Ptacek C. and Blowes D. (2015) Zinc Isotope Fractionation as an Indicator of Geochemical Attenuation Processes. *Environ. Sci. Technol. Lett.* **2**, 314-319.

Wasserman J., Figueiredo A., Pellegatti F. and Silva-Filho E. (2001) Elemental composition of sediment cores from a mangrove environment using neutron activation analysis. *J. Geochem. Explor.* **72**, 129-146.

Weiss D., Rausch N., Mason T., Coles B., Wilkinson J., Ukonmaanaho L., Arnold T. and Nieminen T. (2007) Atmospheric deposition and isotope biogeochemistry of zinc in ombrotrophic peat. *Geochim. Cosmochim. Ac.* **71**, 3498-3517.

Wiederhold J. (2015) Metal Stable Isotope Signatures as Tracers in Environmental Geochemistry. *Environ. Sci. Technol.* **49**, 2606-2624.

Wilkinson J., Weiss D., Mason T. and Coles B. (2005) zinc isotope variation in hydrothermal systems: preliminary evidence from the Irish Midlands ore field. *Econ. Geol.* **100**, 583-590.

Yin N., Sivry Y., Benedetti M., Lens P. and van Hullebusch E. (2016) Application of Zn isotopes in environmental impact assessment of Zn–Pb metallurgical industries: A mini review. *Appl. Geochem.* **64**, 128-135.

Figure Captions

Fig. 1. Map of the study area and location of sampling sites. On the left, it is shown the northeastern shore where are located the main river and channels that discharges into the Sepetiba Bay and the sampling locations of sediments cores at the Saco do Engenhos' mangrove (T1), inner bay area close the mouth of Saco do Engenho (T2) and the mouth of São Francisco Channel (T3).

Fig. 2. Depth profiles of the $\delta^{66}Zn_{JMC}$ values and Zn enrichment factor (Zn EF) of sediment cores.

Fig.3 Depth profiles of Fe/Mn ratios from sediment cores.

Fig. 4. (A) Plot of $\delta^{66}Zn_{JMC}$ values against Zn concentrations of granite rocks, sediment samples, SPM and willemite ores. The dashed squares and the grey rectangles (highlighting the Earth crust) indicate $\delta^{66}Zn_{JMC}$ values of natural and anthropogenic materials reported in the literature for: (i) Earth Crust (+0.28 ±0.05‰, 2σ; Chen et al., 2013); (ii) marine carbonates (from +0.04 to +1.34‰; Kunzmann et al.2013; Pichat et al., 2003); (iii) sewage and wastewater (from +0.08 to +0.31‰; Chen et al., 2009); (iv) metallurgic wastes (generally from +0.59 to +0.81; Jullliot et al., 2011; Sivry et al., 2008); (v) ZnS ores (+0.16 ±0.20‰, 2σ; Sonke et al., 2008); (vi) Zn refined materials (from +0.1 to +0.3; John et al., 2007). (B) The plots of $\delta^{66}Zn_{JMC}$ against enrichment factor (EF) of the core samples and the respective correlation coefficients (R^2).

Fig. 5. Mixing model estimates of the influence of electroplating wastes to determine the zinc concentrations in sediment cores collected at the inner bay. The representative $\delta^{66}Zn$ values of end members are +0.86 ±0.15‰ (2σ) and +0.28 ± 0.12‰ (2σ), for electroplating wastes and continental source (terrigenous materials brought by the rivers), respectively.
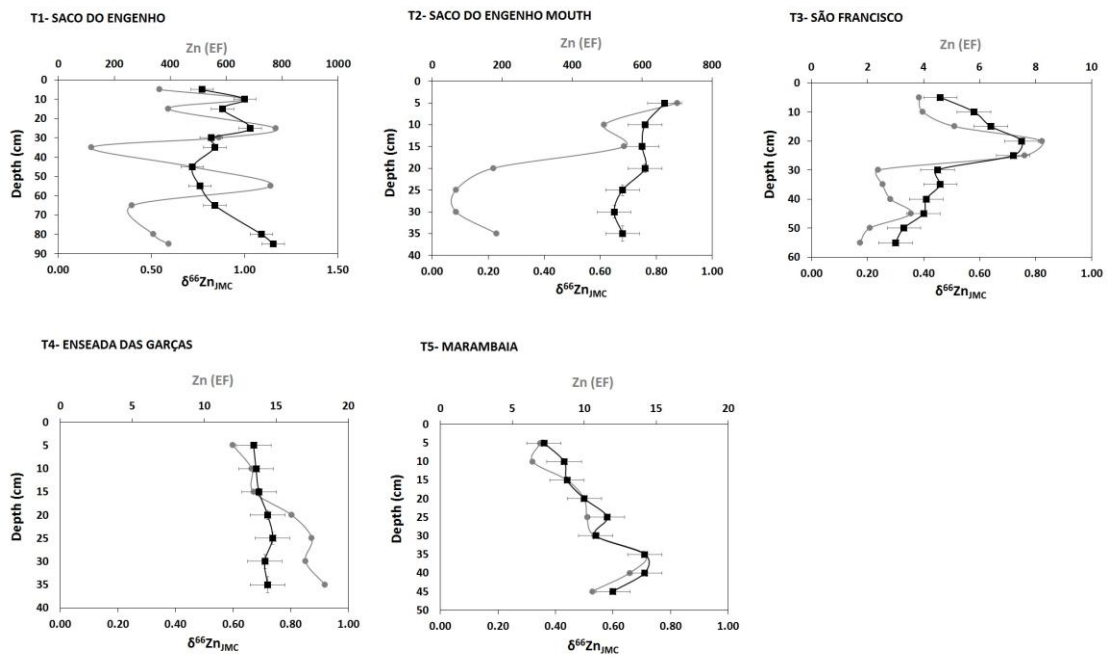
Figure 1

Figure 2

Figure 3

Figure 4
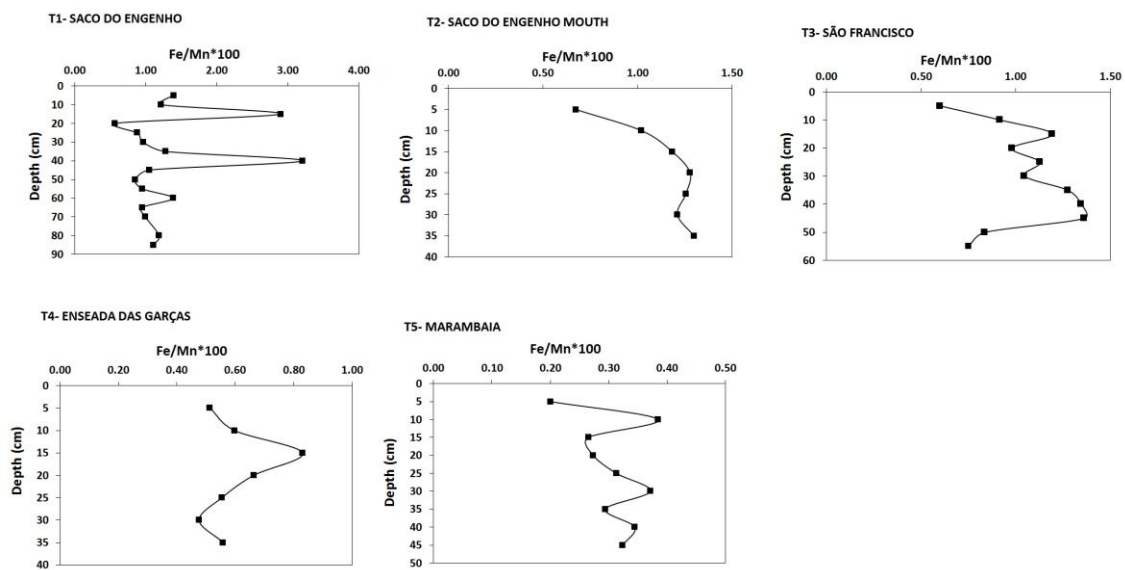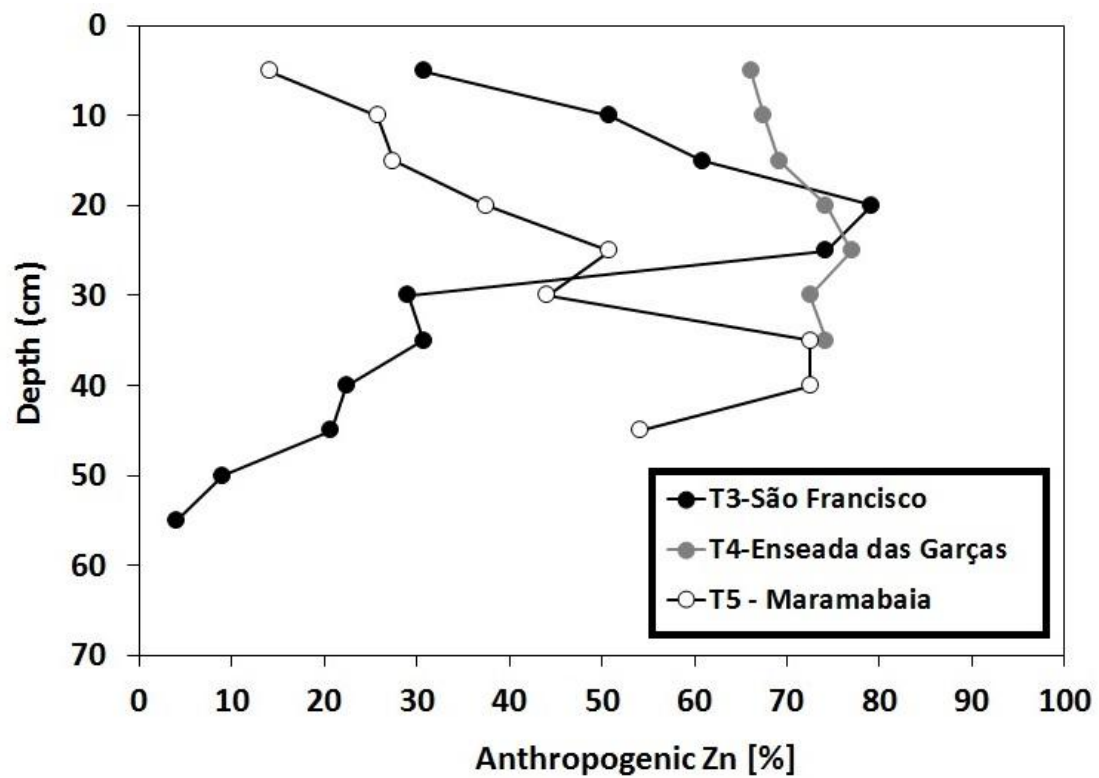
Figure 5
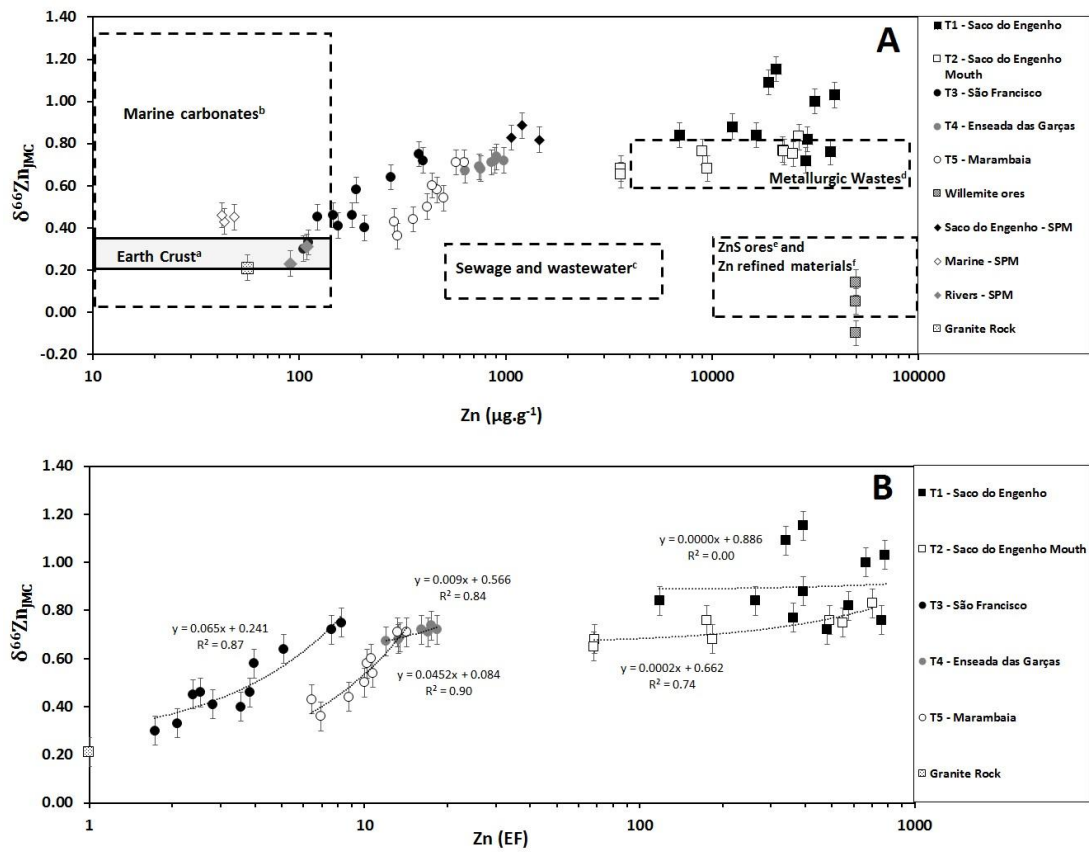
Table 1. Data set of sediment cores, granite rocks and willemite ores samples.

Sample	$\delta^{66}Zn$	Zn EF	Zn ($\mu g.g^{-1}$)	Fe (%)	Al (%)	Mn ($\mu g.g^{-1}$)	Fe/Mn*100
T1 Core- Saco do Engenho							
T1 0-5	0.77	362	21,960	5.1	12.4	369	1.39
T1 5-10	1.00	663	31,410	5.7	9.7	471	1.21
T1 10-15	0.88	394	12,560	6.1	6.5	210	2.90
T1 15-20		208	5,330	1.8	5.3	321	0.57
T1 20-25	1.03	778	39,330	5.9	10.4	677	0.88
T1 25-30	0.82	574	28,980	5.6	10.3	578	0.96
T1 30-35	0.84	118	6,970	5.0	12.1	394	1.27
T1 35-40		204	9,000	12.5	9.0	388	3.21
T1 40-45	0.72	480	28,370	6.6	12.1	632	1.05
T1 45-50		434	22,640	5.6	10.7	659	0.85
T1 50-55	0.76	759	37,540	5.0	10.1	521	0.95
T1 55-60		775	40,400	5.9	10.7	427	1.38
T1 60-65	0.84	264	16,350	5.5	12.7	581	0.95
T1 65-70		789	42,620	5.4	11.1	546	0.99
T1 75-80	1.09	340	18,830	5.5	11.4	463	1.19
T1 80-85	1.15	394	20,470	5.0	10.6	447	1.11
T2 Core- Saco do Engenho mouth							
T2 0-5	0.83	700	26,410	4.4	7.7	654	0.67
T2 5-10	0.76	492	22,360	5.1	9.3	502	1.02
T2 10-15	0.75	549	24,790	4.3	9.3	363	1.18
T2 15-20	0.76	175	8,990	4.6	10.5	364	1.28
T2 20-25	0.68	68	3,610	4.7	10.8	372	1.26
T2 25-30	0.65	68	3,630	4.4	10.9	360	1.21

T2 30-35	0.68	184	9,500	4.7	10.6	362	1.30

T3 Core- São Francisco

T3 0-5	0.46	4	181	4.2	9.7	706	0.60
T3 5-10	0.58	4	189	4.1	9.8	452	0.92
T3 10-15	0.64	5	278	4.8	11.2	402	1.19
T3 15-20	0.75	8	381	4.1	9.5	416	0.98
T3 20-25	0.72	8	397	4.4	10.7	387	1.13
T3 25-30	0.45	2	122	3.4	10.5	328	1.05
T3 30-35	0.46	3	146	3.9	11.8	309	1.27
T3 35-40	0.41	3	155	4.4	11.3	329	1.35
T3 40-45	0.40	4	207	4.7	12.0	341	1.36
T3 45-50	0.33	2	111	4.3	11.0	512	0.84
T3 50-55	0.30	2	105	5.2	12.4	694	0.75

T4 Core- Enseada das Garças

T4 0-5	0.67	12	639	4.7	10.9	924	0.51
T4 5-10	0.68	13	758	4.9	11.7	814	0.60
T4 10-15	0.69	13	747	5.0	11.4	601	0.83
T4 15-20	0.72	16	888	5.2	11.3	788	0.66
T4 20-25	0.74	17	904	5.0	10.6	897	0.55
T4 25-30	0.71	17	852	4.5	10.3	953	0.48
T4 30-35	0.72	18	986	4.7	11.0	839	0.56

T5 Core- Marambaia

T5 0-5	0.36	7	298	3.8	8.8	1,904	0.20
T5 5-10	0.43	6	288	4.1	9.2	1,056	0.38

T5 10-15	0.44	9	356	3.7	8.3	1,409	0.27
T5 15-20	0.50	10	418	4.1	8.6	1,486	0.27
T5 20-25	0.58	10	467	4.2	9.4	1,339	0.31
T5 25-30	0.54	11	501	4.5	9.6	1,215	0.37
T5 30-35	0.71	14	632	4.1	9.1	1,387	0.29
T5 35-40	0.71	13	578	4.2	9.0	1,210	0.34
T5 40-45	0.60	11	442	4.0	8.6	1,221	0.32
Granite	0.21	1	56	4.3	11.5	1,071	0.40

Willemite ores

Willemite 1	-0.10
willemite 2	0.05
willemite 3	0.14

Table 2. Data set of suspended particulate matter (SPM) samples.

	δ^{66}Zn	Zn ($\mu g.g^{-1}$)	Conductivity mS/cm	pH	SPM mg.l^{-1}
SE1	0.88	1207	67.24	8.06	411
SE2	0.82	1455	60.31	8.68	413
SE3	0.83	1063	56. 20	8.33	407
B1	0.43	43	67.38	7.02	177
B2	0.45	48	67.45	8.27	177
B3	0.46	42	67.52	8.20	179
R1	0.31	108	0.08	7.25	278
R2	0.23	90	0.27	6.65	275

Graphical Abstract

Terrigenous materials
$\delta^{66}Zn = 0.28 \pm 0.12‰$

Electroplating wastes
$\delta^{66}Zn = 0.86 \pm 0.15‰$

Diffuse sources: sewage and industrial effluents
$\delta^{66}Zn \approx 0.1 ‰$???

Mixing source processes

Marine materials
$\delta^{66}Zn = +0.45 \pm 0.03‰$